Nanostructured tungsten carbide catalysts for polymer electrolyte fuel cells

X. G. Yang[a] and C. Y. Wang
Electrochemical Engine Center (ECEC), Department of Mechanical Engineering, The Pennsylvania State University, University Park, Pennsylvania 16802

(Received 13 January 2005; accepted 26 April 2005; published online 24 May 2005)

In this study, high current densities (i.e., 0.9 A/cm^2) have been obtained in a hydrogen/air polymer electrolyte fuel cell using nanoscale tungsten carbide as the anode catalyst and carbon supported platinum as the cathode catalyst under normal operating conditions of 80 °C and 3 atm. These results show a possibility of replacing precious metal anode catalysts with transition metal compounds for hydrogen oxidation, thereby creating a fundamental technology to reduce the cost of future fuel cell engines. The tungsten carbide-based catalysts were synthesized by means of chemically reduced mechanical alloying. The high electrocatalytic activity toward hydrogen oxidation reaction is attributed to the inherent W–C valence and the unique nanostructure of synthesized carbides. These properties were confirmed by x-ray diffraction and transmission electron microscopy. © *2005 American Institute of Physics*. [DOI: 10.1063/1.1941473]

Polymer electrolyte fuel cells (PEFCs) are attractive for advanced fuel-efficient vehicles.[1] Key materials in PEFCs include the proton conducting membrane and precious metal catalysts, such as platinum and ruthenium. Unfortunately, the relatively high cost of these materials and insufficient durability are the remaining issues limiting large-scale commercialization of PEFCs. Unlike the membrane electrolyte, the cost of noble metal catalysts will not decline when the future market for fuel cells expands. Reduction of noble metal loading[2] and/or the use of inexpensive alternatives[3] are thus desirable.

There is ample indication that similar to the noble metals, tungsten carbides have many of the desired catalytic properties with respect to hydrogen oxidation and hydrogenolysis reactions, since near Fermi level the electronic density of states of tungsten carbides resembles that of noble metal platinum.[4,5] Fundamental investigations of surface modified C/W(111) or O/C/W(111) also indicated significant catalytic activity toward methanol decomposition to form CO, CH_4, and H_2.[6] Some recent investigations on CO tolerant anode catalysts based upon Pt–Ru/WO_3 (1:0.5:1 by weight)[7] and Pt–Ru–W_2C (1:1:0.4 molar ratio)[8] show improved activity under low voltage polarization in a CO-containing H_2 stream. Another study indicated that a Pt–Ru–WO_3 thin-film electrode, fabricated by sputtering metals onto a WO_3 target as support, showed much higher electro-oxidation current of methanol in a solution of 2.0 M CH_3OH in 0.05 M H_2SO_4, compared to that of Pt–Ru electrodes.[9] The improvement on methanol oxidation is attributed to the ability of WO_2/WO_3 to easily exchange oxidation states by adsorbing hydroxyl ions from water and donating these species to methanol residues adsorbed on Pt.[10]

The same mechanism could explain the improved CO-tolerance of PEFCs with tungsten compound additives. Unlike the strong adsorption of CO on the active Pt sites, the bonding between CO and tungsten carbides is much weaker, allowing the tungsten carbide catalyst high immunity to CO poisoning. One study showed that the presence of CO in the H_2 gas stream causes a minor reduction of 2%–6% in the current from the hydrogen oxidation reaction (HOR) at tungsten carbide electrodes.[11] In the bifunctional electrode Pt–Ru/WO_3/C, the HOR current density was reported as high as 1.6 A/cm^2 at an overpotential of 0.2 V versus reversible hydrogen electrode in the H_2–CO (100 ppm) gases,[7] while the HOR current is <0.5 A/cm^2 for Pt–Ru under similar test conditions. However, there has been much debate as to whether the carbides perform the catalysis in the H_2/CO fuel streams. Furthermore, the mechanism based on weaker bonding cannot provide a full explanation for those experimental results. On the other hand, tungsten carbide shows certain catalytic activity toward HOR. The open-circuit potential for HOR on tungsten carbide is around −0.668 to −0.680 V versus a mercury-mercurous sulphate reference electrode in a 1.5 M H_2SO_4 solution, which closely resembles the H_2/H^+ system. This implies that there is no voltage change in a cell where the Pt anode is replaced by a carbide electrode. Nevertheless, the exact role of tungsten compounds in the electrode reactions remains unclear.

There are no data in the literature regarding the electrode performance of tungsten carbide as the primary catalyst material in PEFCs. In this work, we synthesized nanostructured tungsten carbide-based catalysts (abbreviated as WC-based hereafter), and subsequently fabricated a membrane electrode assembly (MEA) using the synthesized catalysts. Further, we successfully demonstrated high current densities of the resultant MEA in a 5 cm^2 single cell under normal automotive operating conditions. The presence of nanosized WC-based catalyst was confirmed by imaging cross-sectional MEAs with a high-resolution transmission electron microscope. The research finding reported herein is of both fundamental and practical interest.

Nanosized tungsten-based catalyst powders were prepared from a stoichiometric mixture of WO_3, Mg, and C powders (1:6:1 molar ratio) by a mechanical ball-milling process, with milling time typically around 2 days. The milling product was washed with dilute HCl solution to remove the byproduct MgO. This was followed by de-ionized water rinsing and drying in an inert atmosphere at 90 °C.

Several MEAs were fabricated by the decal method using synthesized WC-based catalysts as the anode and carbon supported platinum (Pt/C) as the cathode. Equal weight

[a]Electronic mail: xzy1@psu.edu

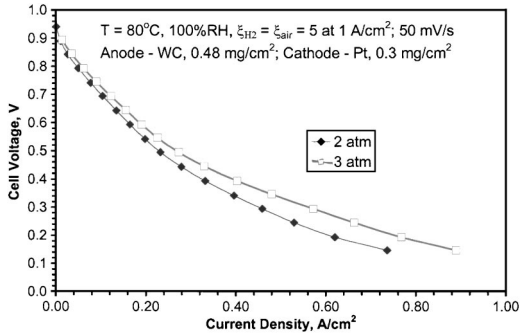

FIG. 1. Polarization curves of the tungsten carbide-based anode in a 5 cm^2 single cell with fully humidified H_2/air at flow rates of 0.2/0.5 slpm and 80 °C.

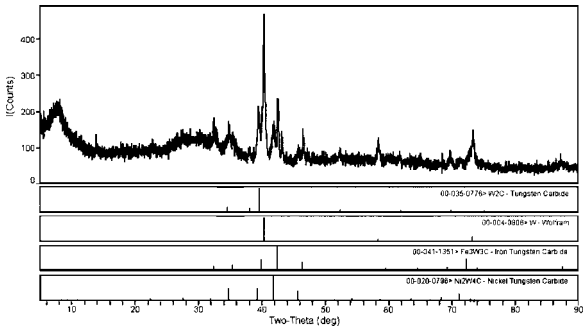

FIG. 2. XRD of the tungsten carbide-based catalysts synthesized by mechanically milling.

amount of WC-based catalyst and carbon powders were mixed with water, Nafion solution (5 wt % Nafion®, equivalent weight=1100), and isopropanol using magnetic stirring. The final ratio of the mixture of (WC+C) to Nafion was 4:1 (by solid weight). The catalyst ink was uniformly applied onto one side of a polytetrafluoroethylene (PTFE) film via the tape casting method. The coated PTFE film was then dried under air. The cathode was prepared by the same method, but using a carbon supported Pt catalyst (40% Pt/Vulcan XC72; E-TEK). The two catalyst-coated PTFE films were hot pressed onto a piece of Nafion® 112 membrane at 125 °C and 100 atm for 3 min. The resultant MEA had a total active area of 5 cm^2, with a catalyst loading of 0.48 mg WC/cm^2 on the anode, and 0.3 mg Pt/cm^2 on the cathode.

Electrochemical performance of the prepared MEAs was evaluated in a 5 cm^2 graphite cell fixture using a fuel cell test stand (Arbin Instruments, College Station, TX) under normal PEFC operating conditions. In assembling the test cell, hydrophobically treated carbon woven cloth coated with a microporous layer (a mixture of PTFE and carbon powder) was employed as the gas diffusion media. The cell temperature was set at 80 °C, and the backpressure was set at 2 or 3 atm (gauge). Hydrogen and air were fully humidified before entering the cell at a flow rate of 0.2 and 0.5 standard liters per minute (slpm), respectively, equivalent to anode/cathode stoichiometry ξ_a/ξ_c of 5, referenced at 1 A/cm^2.

Figure 1 shows the voltage–current polarization curve of the single cell with the WC-based anode under fully humidified H_2/air conditions. The results show that the WC-based anode can provide HOR current densities of 0.7 and 0.9 A/cm^2 at 2 and 3 atm, respectively, with a low WC catalyst loading (~0.5 mg/cm^2). The obtained currents are expected to be anode-limited since the Pt/C cathode is capable of generating 2 A/cm^2 under these test conditions. In comparison with current densities of WC anodes in the literature,[12,13] the HOR current densities of the present WC-based anode are two orders of magnitude higher, and in the range of practical interest to automotive applications. This is the highest electrocatalytic activity of WC-based anodes reported. Further, in this work, the HOR current densities were obtained in a real fuel cell operating under practical conditions, in contrast to the majority of results in the literature which were obtained in electrochemical half cells typically using the rotating-disk electrode technique. The open circuit voltage of the single cell was around 0.95 V, similar to that of Pt-based fuel cells, suggesting both share the same mechanism for HOR. The present data raise a real possibility of replacing Pt-based catalysts with nonprecious metal catalysts, at least for the anode.

The present cell shows a large ohmic loss at high current densities, indicating a high internal resistance. Electrochemical impedance spectroscopy (EIS) was conducted to analyze the sources of the cell resistance using a Solartron 1286 electrochemical interface and 1250 frequency response analyzer, with a perturbation amplitude of 5 mV at 0.85 V over a frequency range of 10 kHz to 0.1 Hz. Impedance measurements were carried out with flow rates of H_2/air =0.08/0.182 slpm under a pressure of 2 or 3 atm. In the conventional Nyquist diagram (Imaginary versus real impedance), the impedance arc is related to ohmic, protonic, kinetic and mass-transport resistances, and capacitances among agglomerates inside the electrodes. In the high-frequency region, the intersection of the EIS spectra with the real axis corresponds to the cell internal ohmic resistance and is estimated to be 0.3 Ω cm^2, which is higher than the 0.1 Ω cm^2 of normal Pt/C MEAs in the same cell fixture. The higher internal resistance is a major factor contributing to the reduced $V-I$ performance of the present cell. For instance, at 0.5 A/cm^2, an increase in the ohmic resistance by 0.2 Ω cm^2 will amount to 0.1 V drop in the $V-I$ curve. An inspection of Fig. 1 clearly reveals that while the catalytic activity of the WC-based anode is impressive, it is still inferior to that of a Pt/C anode. Further optimization of the WC-based anode preparation is thus a goal of future work.

The crystalline structure of the synthesized powders was characterized by using x-ray diffraction at 35 kV (Cu K_α), as shown in Fig. 2. It was found that the synthesized powder is a complex mixture, mainly of hexagonal W_2C and body-centered-cubic plain W, as well as small amounts of hexagonal WC and solid solutions such as W_6Co_6C, W_3Fe_3C, and W_4Ni_2C. Standard x-ray diffraction (XRD) patterns of some main components are also plotted at the bottom of Fig. 2. The impurities such as Fe, Ni, and Co were introduced during the mechanical alloying from the miller.[14] The complex crystalline structures are an inherent feature of mechanical milling technique.[15,16]

In addition to the information about crystallized compounds, the XRD profile contains two halos: one can be seen at $2\theta=8°$, and another spreads over $2\theta=25°-40°$. The halo at the lower angle reflects a structural correlation feature for particles that are nearly periodic in occurrence, with repeat distances near 13 Å (for Cu K_α x-ray radiation). During the XRD measurement, in order to cover the entire surface of the sample, even at lower angles, special techniques including a

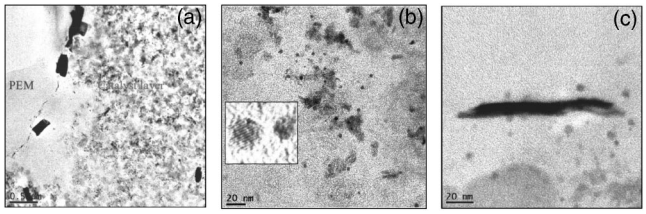

FIG. 3. TEM images of cross section of MEA after electrochemical tests, showing (a): the interface between the polymer electrolyte membrane and the anodic catalyst layer; (b) the presence of nanosized spherical particles; the insert shows a HRTEM image of the crystalline round particles; and (c) irregular flakes of WC-based catalysts, confirmed by EDS.

zero-background holder were used. Therefore, this low-angle halo could not be an instrument artifact. The broad halo at higher angles is generally assigned to the amorphous/nanocrystalline phases.[17]

In order to study the morphology and distribution of catalysts in the anode, we conducted transmission electron microscopy (TEM) imaging of cross-sectional MEA specimens as prepared by ultramicrotomy. Each MEA sample was first embedded in Spurr resin (Electron Microscopy Sciences, Fort Washington, PA) for 24 h at 60 °C. Low embedding temperatures prevent catalyst grain growth and impose less impact on the microstructure of the catalyst layer. Ultrathin sections were cut with glass knives in floating water using a Leica Ultracut E ultramicrotome (Leica, Deerfield, IL). The sections were then transferred to TEM grids. A JEOL 2010 field emission transmission electron microscope was used with an accelerating voltage of 200 kV and point-to-point resolution of 0.19 nm. High-resolution transmission electron microscopy (HRTEM) images and x-ray energy dispersive spectroscopy (EDS) were performed to determine the structural and chemical compositional profiles. All images were recorded with a scanning charge coupled device camera.

Figure 3 shows the TEM images of a cross-sectional MEA after 2 weeks of electrochemical testing. Figure 3(a) depicts the interface between the membrane and the anode catalyst layer. The anode differs from the cathode in terms of the morphology of catalysts, and the presence of tungsten, as well as the absence of platinum in EDS profiles. The membrane can easily be separated out from the resin part with EDS analysis, since the membrane contains significant fluorine while the resin does not. Along the membrane/anode interface, there are some large black blocks (hundreds of nanometers in size), which are identified as plain tungsten. These plain tungsten blocks, also detected by the earlier XRD analysis, lack catalytic activity. Further, the presence of plain tungsten along the interface not only reduces the effective loading of catalysts, but also increases the interfacial resistance between the anode catalyst layer and the membrane. Adding a purification step to exclude plain tungsten will likely improve the overall catalytic activity of the anode in the future.

Inside the catalyst layer, there are irregular pores, indicated as white regions in Fig. 3(a). Pores are knitted into the network for gas transport through the catalyst layer. Small dark catalyst particles are dispersed into a gray matrix of Vulcan carbon powders and/or recast Nafion® ionomer. High-magnification TEM images indicate dispersion of catalyst in at least two kinds of patterns inside the anode: nanosized spherical particles (<5 nm) as shown in Fig. 3(b), and flakes, as shown in Fig. 3(c). These spherical and flake particles could have been formed during the mechanical milling process. Due to the thickness (~ 100 nm) of the TEM specimens, it was difficult to obtain clear HRTEM images of the spherical particles within. Extra TEM specimens were prepared separately using pure catalyst powders to allow observation of subtle microstructural features of the catalysts *ex situ*. The insert of Fig. 3(b) shows the fringe pattern in HRTEM images, indicating the crystalline structure of the spherical particles. EDS revealed that the round particles were made of tungsten and carbon. In addition to the spherical particles inside the anode, there are flake-shaped particles with dimensions of 20 nm long and several nanometers thick. Figure 3(c) also depicts this kind of flake-shaped catalyst in the specimen used for cross-sectional imaging. Again, EDS study indicates that the flakes contain mainly tungsten and carbon, and thus can be considered tungsten carbides.

In this letter, tungsten carbide-based catalysts synthesized by mechanical milling showed a high catalytic activity toward the oxidation of hydrogen. In a 5 $cm^2 H_2$/air PEFC fuel cell, the MEA prepared with synthesized WC-based anode provided a high current density of 0.9 A/cm^2 at 80 °C and 3 atm. These test data have shown the highest electrochemical activity of tungsten carbide catalysts reported to date, and, more importantly, the data were obtained in a real PEFC under automotive operating conditions. As such, the research results described in this letter should be of practical and fundamental interest in the search for nonprecious metal catalysts for fuel cell applications. The electrocatalytic activity of the WC based anode is attributed to the inherent functionalization of tungsten and carbon valence, as well as to the nanostructure, which is capable of providing highly active sites. Work is continuing to further optimize catalyst and electrode preparations in order to demonstrate higher performance of WC-based polymer electrolyte fuel cells.

Support for this work under a Honda Initiation Grant is gratefully acknowledged.

[1] C. Y. Wang, Chem. Rev. (Washington, D.C.) **104**, 4727 (2004).
[2] M. S. Wilson, J. A. Valerio, and S. Gottesfeld, Electrochim. Acta **40**, 353 (1995).
[3] K. Lee, A. Ishihara, S. Mitsushima, N. Kamiya, and K. Ota, Electrochim. Acta **49**, 3479 (2004).
[4] R. B. Levy and M. Boudart, Science **181**, 54 (1973).
[5] J. J. Huang and J. W. Rabalais, Chem. Phys. Lett. **34**, 337 (1975).
[6] H. H. Hwu, J. G. Chen, K. Kourtakis, and J. G. Lavin, J. Phys. Chem. B **105**, 10037 (2001).
[7] K. Y. Chen, Z. Sun, and A. C. C. Tseung, Electrochem. Solid-State Lett. **3**, 10 (2000).
[8] R. Venkataraman, H. R. Kunz, and J. M. Fenton, J. Electrochem. Soc. **150**, A278 (2003).
[9] K. W. Park, K. S. Ahn, J. H. Choi, Y. C. Nah, and Y. E. Sung, Appl. Phys. Lett. **82**, 1090 (2003).
[10] S. Arico, S. Srinivasan, and V. Antonucci, Fuel Cells **1**, 133 (2001).
[11] D. R. McIntyre, G. T. Burstein, and A. Vossen, J. Power Sources **107**, 67 (2002).
[12] C. J. Barnett, G. T. Burstein, A. R. J. Kucernak, and K. R. Williams, Electrochim. Acta **42**, 2381 (1997).
[13] S. Bodoardo, M. Maja, N. Penazzi, and F. Henn, Electrochim. Acta **42**, 2603 (1997).
[14] G. M. Wang, S. J. Campbell, A. Calka, and W. A. Kaczmrek, J. Mater. Sci. **32**, 1461 (1997).
[15] F. L. Zhang, C. Y. Wang, and M. Zhu, Scr. Mater. **49**, 1123 (2003).
[16] G. L. Tan and X. J. Wu, Powder Metall. **10**, 300 (1998).
[17] L. Gao and B. H. Kear, Nanostruct. Mater. **5**, 555 (1995).